



# Harnessing $\alpha\beta$ T cell receptor mechanobiology to achieve the promise of immuno-oncology

Ellis L. Reinherz<sup>a,b,c,1</sup> , Wonmuk Hwang<sup>d,e,f,1</sup> , and Matthew J. Lang<sup>g,h,1</sup>

Edited by Bert Vogelstein, Johns Hopkins University, Baltimore, MD; received December 7, 2022; accepted May 19, 2023

T cell receptors (TCR) on cytolytic T lymphocytes (CTLs) recognize "foreign" antigens bound in the groove of major histocompatibility complex (MHC) molecules (H-2 in mouse and HLA in human) displayed on altered cells. These antigens are peptide fragments of proteins derived either from infectious pathogens or cellular transformations during cancer evolution. The conjoint ligand formed by the foreign peptide and MHC, termed pMHC, marks an aberrant cell as a target for CTL-mediated destruction. Recent data have provided compelling evidence that adaptive protection is achieved in a facile manner during immune surveillance when mechanical load consequent to cellular motion is applied to the bond formed between an  $\alpha\beta$  TCR and its pMHC ligand arrayed on a disease-altered cell. Mechanobiology maximizes both TCR specificity and sensitivity in comparison to receptor ligation in the absence of force. While the field of immunotherapy has made advances to impact the survival of cancer patients, the latest information relevant to T cell targeting and mechanotransduction has yet to be applied for T cell monitoring and treatment of patients in the clinic. Here we review these data, and challenge scientists and physicians to apply critical biophysical parameters of TCR mechanobiology to the medical oncology field, broadening treatment success within and among various cancer types. We assert that TCRs with digital ligand-sensing performance capability directed at sparsely as well as luminously displayed tumor-specific neoantigens and certain tumor-associated antigens can improve effective cancer vaccine development and immunotherapy paradigms.

immuno-oncology | T cell receptor | mechanobiology

Treatment of cancers has improved through immunotherapy, an approach that uses the immune system to control and eliminate cancers (1). Breakthroughs have been particularly evident in malignant melanoma where treatments with anti-PD1 and/or anti-CTLA4 monoclonal antibodies rejuvenate dormant T lymphocytes within the tumor site by abrogating inhibitory pathways, so-called immune checkpoint blockade therapy (CB). Cancers responsive to CB such as melanoma and a fraction of non-small cell lung cancers (NSCLCs) (20%) display myriad tumor-specific antigens, "neoantigens", to stimulate the immune response (2). Neoantigens arise most commonly through genetic mutations in a tumor. Cytolytic T lymphocytes (CTLs) are generated naturally against some of these neoantigens, following the priming of naïve T cells by professional antigen presenting cells (APCs) that then target the cancer for destruction once the tumor's checkpoint evasion mechanism has been eliminated. However, for many other forms of cancer including the remaining 80% of NSCLCs, almost all ovarian

cancers, and brain cancers, to mention a few, the paucity of neoantigens arrayed on the tumor cell prevents the immune system from effectively generating CTLs in the first instance. Unsurprisingly, no positive response is engendered by CB. Mechanisms of tumor evasion that thwart protective immunity are known, including genetic and epigenetic restriction of antigen display, inhibitors of T cell migration and induction of T cell exhaustion via metabolites and/or chronic antigen stimulation in the tumor microenvironment (3–5).

Several approaches are currently being tested to overcome the problem of dysfunctional effectors including the search for additional CB pathways and clinical trials of mAb combinations incorporated in a neoadjuvant setting prior to surgery (6, 7). In one orthogonal strategy, a chimeric antigen receptor is introduced into T cells (CAR-T) by lentiviral or other retroviral transduction to bind to and destroy tumor cells (8). CAR-T therapy incorporates an antibody fragment specific for a tumor-specific antigen or tumor-associated antigen (TAA) joined to a CD3 signaling subunit component via a linker and transmembrane (TM) region of another protein (*SI Appendix, Fig. S1A*). Another strategy to induce killing employs a bispecific antibody fusion protein comprising two single chain variable fragments (scFv), diabodies that engage nearby T cells via CD3 with one arm and a tumor cell target with the other (9). Each has merit with remarkable successes emerging at various preclinical and/or clinical stages. Notwithstanding, costs for therapies like CAR-T are very high, and benefits to some patients may be transient due either to tumor target antigen loss driven by immune selection or, alternatively, exhaustion of CAR-T function (8).

Importantly, ongoing immunotherapy efforts have yet to benefit from recent scientific advances in fundamental T cell receptor (TCR) structural biology and antigen-specific cognate

Author affiliations: <sup>a</sup>Laboratory of Immunobiology, Dana-Farber Cancer Institute, Boston, MA 02115; <sup>b</sup>Department of Medical Oncology, Dana-Farber Cancer Institute, Boston, MA 02115; <sup>c</sup>Department of Medicine, Harvard Medical School, Boston, MA 02115; <sup>d</sup>Department of Biomedical Engineering, Texas A&M University, College Station, TX 77843; <sup>e</sup>Department of Materials Science and Engineering, Texas A&M University, College Station, TX 77843; <sup>f</sup>Department of Physics and Astronomy, Texas A&M University, College Station, TX 77843; <sup>g</sup>Department of Chemical and Biomolecular Engineering, Vanderbilt University, Nashville, TN 37235; and <sup>h</sup>Department of Molecular Physiology and Biophysics, Vanderbilt University School of Medicine, Nashville, TN 37235

Author contributions: E.L.R., W.H., and M.J.L. wrote the paper.

The authors declare no competing interest.

This article is a PNAS Direct Submission.

Copyright © 2023 the Author(s). Published by PNAS. This open access article is distributed under [Creative Commons Attribution-NonCommercial-NoDerivatives License 4.0 \(CC BY-NC-ND\)](https://creativecommons.org/licenses/by-nc-nd/4.0/).

<sup>1</sup>To whom correspondence may be addressed. Email: ellis\_reinherz@dfci.harvard.edu, hwm@tamu.edu, or matt.lang@vanderbilt.edu.

This article contains supporting information online at <https://www.pnas.org/lookup/suppl/doi:10.1073/pnas.2215694120/-/DCSupplemental>.

Published June 20, 2023.

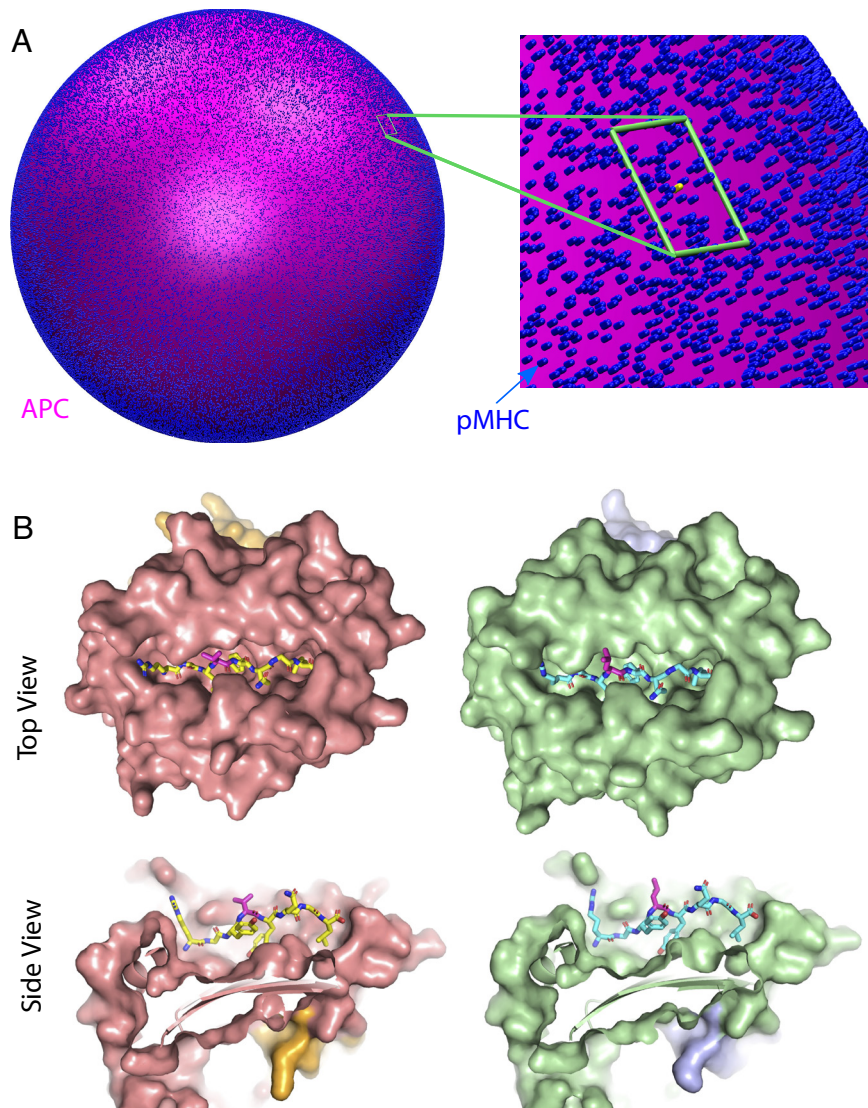


**Fig. 1.** Immune surveillance: an exacting search for a needle in a haystack. (A) A cell expressing approximately 100,000 pMHC complexes of various types (diverse peptides and MHC allele products) shown schematically as blue molecules arrayed on the surface. A magnified view around the boxed region shows a single yellow dot representing a copy of a rare “foreign peptide”, i.e., neoantigen or virus-derived peptide that could be targeted by a CTL for destruction. (B) 2 pMHC complexes that are almost identical except for a focal change at the p4 position of the peptide (RGYVYQGL vs. RGYLYQGL) bound to H-2 K<sup>b</sup> that an N15 TCR distinguishes (see text). Top views of antigen-binding groove of pMHC molecule VSV8/K<sup>b</sup> (Left) and L4/K<sup>b</sup> (Right) are shown from the perspective of an approaching TCR (Upper row). (Left) MHC K<sup>b</sup> is shown in surface representation with the heavy chain colored in salmon while  $\beta_{2m}$  is in pale yellow. VSV8 peptide is in stick representation with its N terminus on the left and C terminus on the right. The Val residue at p4 is highlighted in magenta. (Right) MHC K<sup>b</sup> is shown in surface representation with the heavy chain colored in pale green and  $\beta_{2m}$  in light blue. The L4 peptide is drawn similarly in stick representation. The Leu residue at p4 of the L4 peptide is highlighted in magenta. In the Bottom row, the corresponding side cross-sectional views of the antigen-binding groove of pMHC molecules are offered with peptides in same left to right orientation.

recognition of the  $\alpha\beta$  T cell lineage. TCRs with digital performance characteristics (i.e., requiring only one or a few, countable ligands for activation) directed at physically detected neoantigens can change cancer vaccine and immunotherapy paradigms, by targeting tumors via sparsely as well as luminously arrayed TAAs (10–12). The purpose of this Perspective is to make clinicians and basic life scientists aware of  $\alpha\beta$ TCR features that arose through ~400 My (million years) of jawed vertebrate evolution. Such comprehension allows for formulation of rational therapeutic options. Precise CTL targeting can avoid autoimmune inflammatory toxicities induced by CB therapy (13). Although we focus on CD8<sup>+</sup> CTLs, CD4<sup>+</sup> helper T cells use the same structural features to exploit mechanobiology (14, 15).

### A Fundamental Conundrum: How Can Weak $\alpha\beta$ TCR Binding Mediate Exquisite In Vivo Specificity and Sensitivity?

Paucity of tumor target antigens discussed above refers both to the absence of more than 90% of bioinformatically predicted neoantigen candidates on the tumor cell surface and, even when displayed, presentation in limited copy numbers.

Consequently, only several molecules per cell are expressed among a sea of normal self-peptides (~100,000) (9, 16). The discernment process from the CTL’s perspective (Fig. 1A) is really a search requiring detection of a needle in a haystack. As each CTL carries 20,000 to 40,000 identical clonotypic TCRs, multiple parallel confinement area searches are possible at the CTL–tumor cell interface. Nevertheless, the explanation for how a TCR, a class of receptor with micromolar or weaker affinity for ligand, can accomplish this arduous task was obscure. Additionally perplexing has been the extraordinary selectivity of peptide recognition. For instance, Fig. 1B shows crystal structures of two foreign peptide and MHC ligands (pMHC) that differ at a single p4 residue of the peptide. Only a small number of atoms are distinct and yet a specific TCR can handily identify one from the other with a biological response that diverges 10,000-fold (17).

During lymphocyte development, self-reactive cells are eliminated to prevent autoimmunity (18, 19). Nonetheless, mature T cell recognition of a foreign peptide involves ligation of that peptide bound to a self-MHC (major histocompatibility complex) molecule. As shown in Fig. 2A, the pMHC mosaic comprises a small number of foreign peptide residues embedded within many more “self” MHC residues. This creates a

tricky proposition since most of the TCR recognition surface interacts directly with a self-constituent. In contrast, the surface B cell receptor (BCR) and that of its secreted antibodies generally recognize an entirely foreign antigen. Furthermore, B cells undergo somatic hypermutation of their immunoglobulin genes in the lymph node and spleen to enhance affinity for ligand (20). This refinement mechanism is not operative for TCR genes because it would foster self-MHC reactivity that could result in autoimmunity. Following somatic hypermutation, antibody affinity can achieve equilibrium K<sub>d</sub> values of nM-pM while αβTCR values are orders of magnitude weaker, in the 1 μM to 100 μM range. How then can T cells manifest the specificity and sensitivity required to recognize a single pMHC molecule on the surface of a target cell (21)?

The answer is that the αβTCR is a mechanosensor, a biomolecule that discerns a change in force upon ligation (10, 22–29). Force is placed on an individual bond formed between αβTCR and pMHC consequent to cell motion during immune surveillance. This bond works like a sailor's bowline knot which is secure under load but easy to work free, untie or slip, when not under tension. Fig. 2B shows a force-bond lifetime curve for two TCRs that recognize the same pMHC. At low or no force, binding to specific and irrelevant pMHC molecules is comparably weak. In contrast, bond lifetime becomes highly specified at a 10- to 15-pN force. Note that these two TCRs interact with the same pMHC but manifest different bond lifetimes. Upon binding to the pMHC each TCR undergoes conformational changes including extensions in the bound state. Initially, a TCR is in a compact state but then transitions to an elongated state while bound to pMHC (Fig. 2C). At this point, the interaction can break (Fig. 2C) or transition back and forth (Fig. 2D) as if in a resonant state. The extension distance, force, and the transition frequency of each TCR can vary. Such motions induced via an optical trap recapitulate the native

loading condition generated by the actin–myosin machinery in a T cell in contact with an APC. Physiological tangential force applied as T cells migrate across stroma and APCs in tissues is exploited for mechanosensing, as seen in optical tweezers experiments where applying forces that are tangential rather than normal to the membrane led to T cell activation (10, 23). Parameters describing these motions and downstream signaling events are detailed below.

As a TCR undergoes transitions, it tugs at the membrane of the T cell, delivering energy to generate signal through perturbation of vicinal lipids and facilitating exposure of the cytoplasmic signaling motifs of the CD3 subunits, termed ITAMs (immunoreceptor tyrosine-based activation motifs) (SI Appendix, Fig. S1B). Consequent downstream gene transcription occurs through a multicomponent relay (30). One may envision this process as switching between a resting and signaling-competent state driven by an attowatt generator (force\*distance\*frequency = 15 pN\*10nm\*1/s = 1.5\*10<sup>-19</sup>J/s = 0.15 aW). Biophysical distinctions among TCRs, even when directed at the same pMHC ligand, lead to signaling differences. These involve dynamic structural changes in the recognition surface of the TCR and its constant region module as well as the surrounding six invariant CD3 signaling components (CD3εγ, CD3εδ and CD3ζζ) associated with the TCRαβ clonotype (clone-specific heterodimer) that binds pMHC (SI Appendix, Fig. S2) (25, 31). Unlike soluble antibodies, the αβTCR transcends simple binding, functioning out of equilibrium in an energized state.

## Biophysics of TCRs and preTCRs in the αβ Lineage vs. TCRs in the γδ Lineage

**Catching a Bond in the αβ Developmental Pathway.** Direct biophysical probing of the αβTCR-pMHC revealed unique mechanosensing features including catch bond profiles

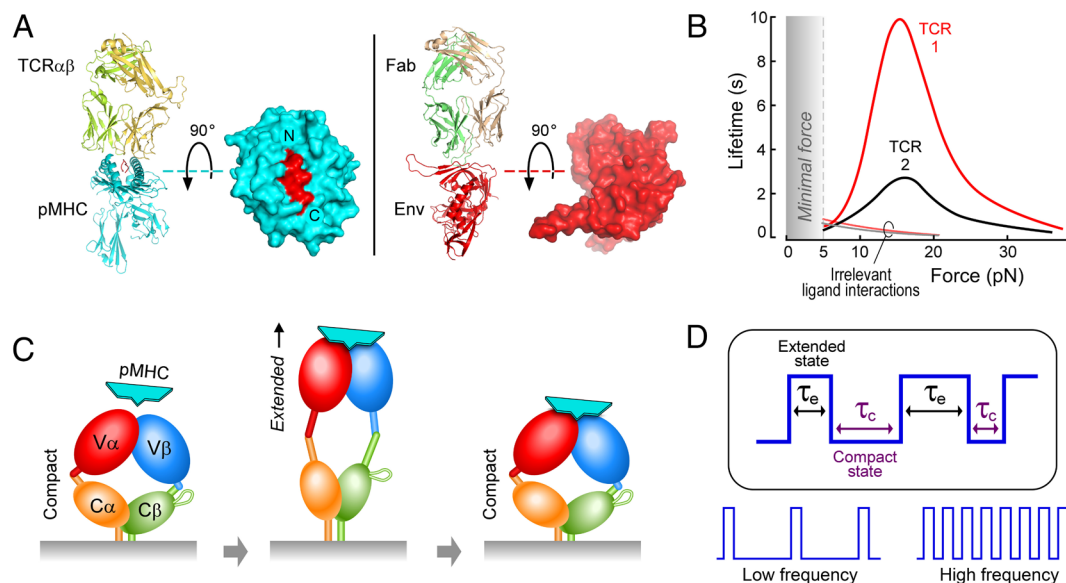


**Fig. 2.** αβ T cell recognition via mechanosensing. (A) X-ray structures of TCRαβ recognizing an influenza A virus M1 peptide bound to the HLA-A\*0201 (PDB 1OGA) in comparison to a human immunoglobulin Fab fragment bound to HIV-1 gp120 core (PDB 1GC1). For each, a ribbon diagram of the receptor structure (Left, side view) and a surface model of the respective ligand (Right, 90° rotation) are shown with the foreign protein-derived element in red. The peptide in the pMHC is size-wise a minor component of the interaction surface. N and C mark the amino and carboxy terminus of the foreign peptide. The red peptide chain is barely visible in the side view between the MHC α-helices (cyan). (B) Force-bond lifetime curves of two distinct TCRs (1 and 2) interacting with the same pMHC cognate ligand or irrelevant peptide. (C) Structural transitions following TCR binding to pMHC. In this cartoon, only the TCRαβ variable and constant domains are shown for simplicity. The TCR view in panel A is rotated upside down, which is utilized in subsequent figures. (D, Top) Reversible transitioning between extended and compact states with indicated time constants as an example of one mechanotransduction parameter. (Bottom) low and high transition rates of two distinct TCRs.

and conformational transitions. Measurements performed on cells and purified components with optical tweezers (22, 24–26) and bioforce probe methods (27–29) demonstrate a catch bond where the bond lifetime initially increases with load and then weakens, with a peak lifetime occurring at 15- to 20-pN force (22, 24). During immune surveillance, such forces naturally arise from cell motions that involve the cell's peripheral actin network. The peak lifetimes generally range ~1 to 10 s depending on the system and ligand potency. Optical tweezer measurements also show discrete conformational transitions under load including small nm-level motions and a large (and reversible) signature conformational change at 15 pN (Fig. 2 B–D)

Why a catch bond? While the bond lifetime increases with force, it is still modest compared to other high-affinity interactions such as those seen with typical antibody–antigen binding. Thus, it is unlikely that the lifetime per se drives signaling. More importantly, the 15-pN force at the peak catch bond lifetime can drive molecular motions and conformational transitions that would otherwise be inaccessible in a nonenergized state. The energy associated with signature conformational change (15 pN\*10 nm) is significant, in fact equivalent in magnitude to the free energy associated with ATP hydrolysis if only half of that transition is utilized (15 pN\*5 nm = 75 pN\*nm). From a nonequilibrium perspective, the system is normally in a resting, i.e., “off” state, and it is gated only when force is introduced. Surmounting the barrier through thermal energy alone is 90 million times less likely [ $\exp(-75/4.1)$ ] than pulling with an external force through a cognate ligand (*SI Appendix, Text S1*). Such a change thus requires energy input. A catch bond enables energy delivery and drives the system over the energy barrier to a signaling competent state. This scenario also supports the kinetic proofreading mechanism where the fidelity of signaling is enhanced by combining apparently error-prone kinetic events with the supply of free energy (32).

The T cell activation process begins with a loaded state spanning the T cell and APC through their respective assembled actomyosin cytoskeletal machineries. On T cells, actin-rich membrane protrusions, microvilli, studded with surface TCRs are facilitative. The attendant motions pulling across the cell–cell interface provide sufficient energy to drive signaling. In contrast, thermal energies are insufficient to surmount this barrier. The load activates the TCR–pMHC catch bond (31), which in turn induces the conformational change. We believe that the energy associated with the conformational transition drives the TM domain structural rearrangements including a toggle in the  $\alpha$  TM domain that leads to dissociation of CD3 $\zeta\zeta$  releasing membrane sequestered ITAMs (25). This event appears to be coupled to motor proteins that turn on locally and transport the ligated TCR to follow the force, maintaining an optimal load needed for reversible conformational change and continued signaling. At the same time, unligated TCRs adjacent to the ligated TCR are translocated by motors to initiate immunological synapse (IS) formation as well (10). This spatial reorganization of individual molecules revealed by pointillist data (33) plausibly promulgates effective signalsome formation and segregates phosphatases away from relevant activating kinases such as Lck for phosphorylation of accessible ITAMs in early T cell activation. In our experiments, at low pMHC interfacial

density this load bearing pathway is reproduced from force on the bead through the optical trap. At higher interfacial density, where force is not required for activation, akin to APCs arraying hundreds or more copies of a pMHC at the T cell–APC interface, T cell machinery may be able to organize sufficiently through multiple pMHC locations to pull through the bead and initiate the same downstream signaling pathways.

The preTCR, which is present during  $\beta$  selection, also contains mechanosensing features (24). The preTCR in many ways is a simpler system since a clonotypic  $\beta$  subunit is paired through its constant domain with preTCR  $\alpha$  (pT $\alpha$ ), an invariant TCR $\alpha$  surrogate lacking a V domain (24, 34–37). The pT $\alpha$ – $\beta$  heterodimer associates with the same set of CD3 subunits as found in the  $\alpha\beta$ TCR. Pulling through pMHC occurs exclusively via the unpaired V $\beta$  domain and exhibits a more complex catch bond profile than that of the TCR $\alpha\beta$  paired V $\alpha$ V $\beta$  module and a 10-fold increase in the rate of reversible hopping of the signature conformational transition. By mapping the forward and reverse rates as a function of force, it was determined that the critical force is similar between the preTCR–pMHC and TCR $\alpha\beta$ –pMHC systems implying that the structural transition is associated with the shared  $\beta$  subunit (24, 26). Hyperactive transitioning and broader peptide specificity of a preTCR (relative to TCR $\alpha\beta$ ) during  $\beta$  selection favor signaling (24, 36) to expand the  $\beta$  chain repertoire preceding  $\alpha\beta$ TCR expression while limiting cellular plasticity to facilitate normal thymocyte development (38). These mechanisms anticipate subsequent  $\alpha\beta$ TCR-driven winnowing of the mature T cell repertoire linked to thymic positive and negative selection.

**$\gamma\delta$ TCRs Are Not Mechanosensors.** Further insight on the importance of mechanosensing in the T cell lineage came from a study comparing a  $\gamma\delta$ TCR to an  $\alpha\beta$ TCR and a V $\gamma$ V $\delta$ –C $\alpha$ C $\beta$  chimeric receptor (12). The latter amalgamated the variable domains of the  $\gamma\delta$ T cells with the constant domains of the  $\alpha\beta$ TCR.  $\gamma\delta$ T cells are found in barrier tissues and recognize plentiful nonpeptide ligands induced on stressed cells targeted for destruction (39). Like antibody Fabs,  $\gamma\delta$ TCRs lack both the extended constant  $\beta$  domain connector between the F and G strands (FG-loop) and a sizeable interfacial contact area between the constant and variable domains, distinguishing features of  $\alpha\beta$ TCRs (*SI Appendix, Figs. S1 D and E and S2A*).  $\gamma\delta$ TCR–pMHC interactions were slip bond-like, where the bond lifetime decreases exponentially with applied force. In contrast, the chimera showed a catch bond even though both receptors have the identical V module interacting with the same ligand sulfatide–CD1d, a sulfolipid bound to a class Ib MHC molecule. Conformational changes were also readily observed in the chimera but not in the  $\gamma\delta$ TCR.

**Analogue vs. Digital Performance.** The adaptive immune system must perform effectively with plentiful as well as sparse ligands. To map the chemical and physical requirements for the breadth of response capability, we trapped beads coated with different numbers of a given pMHC molecule and apposed them to a T cell to facilitate activation. A sufficiently large number of pMHC molecules can activate a T cell without any external force. Here, we believe internal cellular machinery/motions stabilize and

pull across the bead itself through multiple pMHC bond locations, eliminating the requirement for an external force. We refer to this as an “analog” response. In addition to  $\gamma\delta$ T cells operating under these analog conditions where stress response ligands are plentiful, some  $\alpha\beta$  T cells, including those directed at highly arrayed viral antigens such as the nucleoprotein epitope of influenza A viruses (NP<sub>366-374</sub>), do not require sparse ligand detection capability (40). Our bead-facilitated activation study also demonstrates that with an optimal balance of ligand and external force, a subset of T cells can perform “digitally,” triggering reliably with as few as two pMHC molecules at the bead–T cell interface (10). Such activation requires force from the optical trap, however, and is tightly centered around 15 pN. This digital T cell triggering is tied to the actomyosin machinery that sustains the force in this window where signaling is optimal (10) and in vivo likely induces IS formation through recruitment of nonligated TCRs noted above. Defining those digital-quality TCRs that recognize a given pMHC among an individual’s repertoire of TCRs recognizing the same ligand shall be advantageous for vaccination purposes and adoptive immunotherapy.

**Systems Biomechanics.** Cells continually reorganize their internal components, changing shape, and exerting forces on and responding to their surroundings through dynamic interfacial contacts (Fig. 3). This is powered by a network of cellular components, stroma and conduits, collectively a cellular power grid, which delivers energy to drive signaling. The ability of cells to bend various force probes and push/pull on other model APC surfaces (41–47) demonstrates that sufficient forces are available for individual receptor activation as shown by careful measurements at the single molecule level (*SI Appendix, Text S2*). Coupling to the grid is also influenced by local stiffness of the microenvironment, which can change dramatically during processes such as inflammation and cancer (48, 49). Stiffness, a measure of deformation under a given load on a material, can vary 100 fold under physiological (compliant) vs. inflammatory (stiff) conditions in the same tissue, and it varies even more in different tissues such as compliant bone marrow and brain vs. stiff cartilage and bone (50). The immune system adapts itself to function in the range of organ-related locales of the mammalian organism.

TCRs may exploit different optimal force parameters when operating on T cells in compliant as opposed to stiff tissues in anatomically linked locales, for example, a mediastinal lymph node draining intraepithelial and subendothelial surfaces of the lung as pictured at the *Top* of Fig. 3 (*Left* and *Right*, respectively). Furthermore, interplay between cancer cells and the tumor microenvironment often increases stiffness of the extracellular matrix (ECM), impacting optimal TCR mechanobiology. T cells produce many mediators which in turn modulate the ECM and its stiffness (48, 49). For example, TGF- $\beta$  and TNF- $\alpha$  enhance or inhibit fibroblast collagen biosynthesis, respectively. The quality of a TCR that reacts with a neoantigen and its downstream transcriptome following ligation is likely to differentially regulate responsiveness to the tumor while at the same time modulating ECM mechanics and the tumor microenvironment more broadly, impacting productive T cell activation vs. exhaustion.

Within the T cell itself, activation is coupled to an intracellular motility system, providing further points of modulation

and control (10). This internal system must work near the activation threshold yet be robust enough to handle a wide range of inputs such as a sparse vs. plentiful pMHC ligand and a stiff vs. a compliant microenvironment. In some cases, internal cytoskeletal machinery may not be preassembled and/or properly connected to the TCR complex, reducing competence to drive receptor inputs. In other cases, organized machinery and coupling may be fully primed at the interface of a mature dendritic cell and a naïve T cell within an ideal microenvironment prearranged to foster signaling events linked to relevant biomechanics (10). There must be a delicate balance between external drivers including dynamic microenvironment stiffness and internal machinery that a T cell integrates.

How does our immune system dampen T cell activation? If T cells fire too readily in response to ligand, there is excessive noise. Conversely, if activation thresholds are set too high, a rare signal will not be detected. The adaptive T cell response must therefore strike a critical balance between extremes. Perhaps acute inflammation in a microenvironment can shift the set point to where signal levels are being heard even if weak, analogous to a squelch in an electronic circuit that adjusts output based on signal strength. Within a perfect microenvironment and a carefully matched signal frequency such as in the lymph node where naïve T cells and APCs prime the immune response, a true digital channel can come in loud and clear. In contrast, chronic inflammation including that found in the tumor microenvironment may pose challenges, which may be overcome by recruitment of high-“acuity” T cells with potent digital responses enabled to function at requisite bioforces mandated by the mechanics of the system.

## Atomistic Basis of Catch Bond Formation

Since the mechanosensing action of an  $\alpha\beta$ TCR is a nonequilibrium process, static X-ray crystallographic structures of TCR $\alpha\beta$ –pMHC complexes cannot populate all energized states to reveal the clear cognate antigen recognition mechanism (51). While the activation of a T cell upon recognizing the matching pMHC is a multistep process (52), mechanosensing starts with the engagement of the TCR $\alpha\beta$  heterodimer by its cognate pMHC, as shown in in vitro single-molecule experiments of isolated TCR $\alpha\beta$ –pMHC complexes without coreceptors (22). This engagement involves two elements, catch bond formation and conformational transition as noted above. The former is required for the latter and is then followed by pMHC-mediated T cell activation. An example of catch bond being necessary but not sufficient for T cell activation is the experiment where the C $\beta$  FG-loop (*SI Appendix, Fig. S2A*) is stabilized by the H57 antibody. It drastically enhanced the peak catch bond and the bond lifetime but blunted the structural transition and associated T cell activation (10). This study also demonstrated how allostery controls binding between TCR $\alpha\beta$  and pMHC (22). Further confounding is the fact that TCR $\alpha\beta$  characteristically forms more contacts with the MHC molecule than the antigenic peptide (Fig. 2A), making it difficult to understand how the catch bond behavior is controlled via a handful of peptide contacts, while possessing a very weak equilibrium binding affinity.

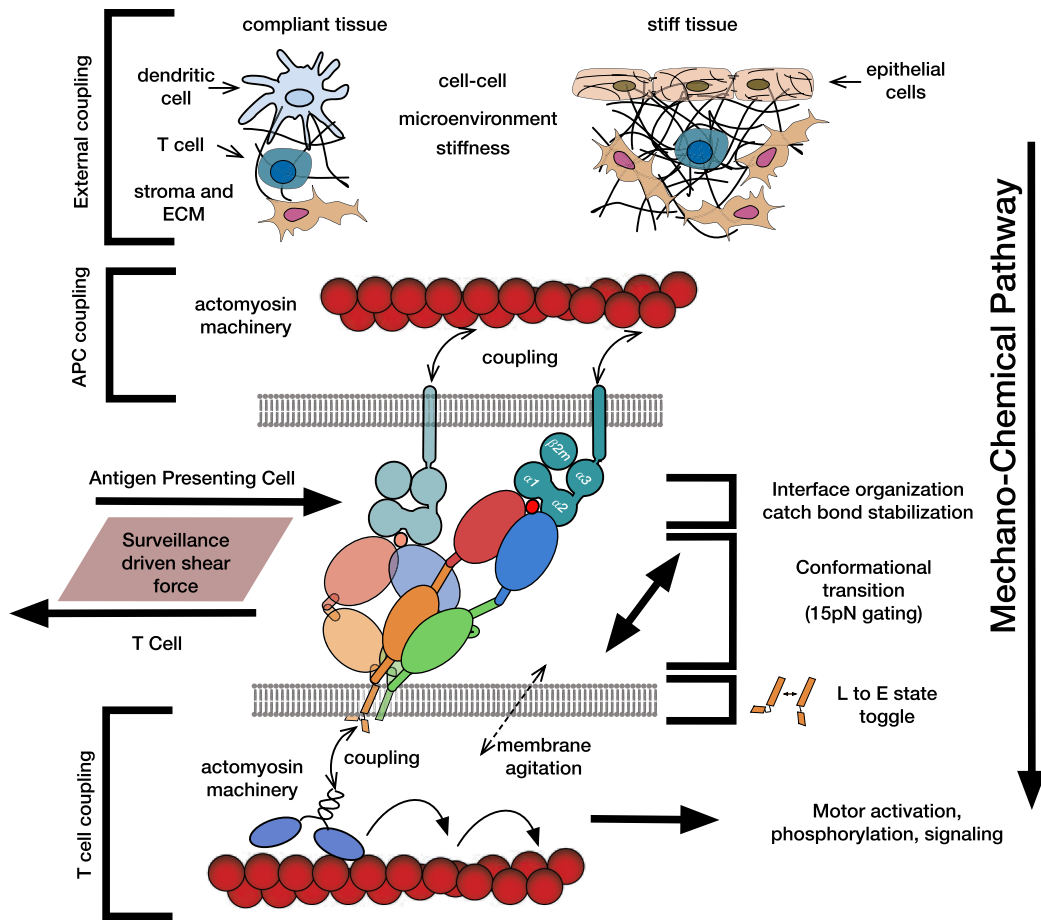


**Fig. 3.** Systems view of the  $\alpha\beta$ TCR mechanome. Stiffness of the cellular microenvironment modulates mechanical coupling between T cells and APCs (External coupling to the grid shown at the top of the figure). Local compliance ranges two orders of magnitude, about  $\sim 1$  to  $100$  kPa, and is substantially altered in inflamed, infected, or diseased tissues. Such changes fine-tune signaling levels during immune surveillance. Differences in compliance of anatomically linked locals as discussed in the text are shown with some key cell types labeled and ECM components represented as wavy lines. The other figure elements depict the mechanochemical pathway that works through the  $\alpha\beta$ TCR-pMHC bond connecting across the active and load bearing actomyosin machinery in both the APC and T cell as denoted. During surveillance, shear forces exert on cell surfaces, tilting the  $\alpha\beta$ TCR-pMHC bond (TCR $\alpha\beta$  alone shown for simplicity). Interfacial organization and catch bond stabilization occurs between pMHC and the variable domains of  $\alpha\beta$ TCR. Force strengthens the bond, extending the lifetime and energizing the system. This input facilitates a  $\sim 10$ -nm conformational transition that is inaccessible by thermal fluctuation alone. Reversible transitioning agitates the T cell membrane toggling the TCR $\alpha$  transmembrane domain from bent (L) to extended (E) conformations. Such agitation and motion loosens the transmembrane helix organization leading to the release of membrane-sequestered CD3 ITAM domains (omitted for clarity). Internal coupling to the actomyosin machinery maintains the load between the APC and TCR at the proper level for reversible transitioning.

Our all-atom molecular dynamics (MD) simulation study revealed a dynamic mechanism of catch bond formation (Fig. 4) (31). The 4-domain organization in a rhomboidal topology provides room for fine-tuning mechanical properties of the TCR $\alpha\beta$  heterodimer to improve interfacial mismatches. The number and organization of interfacial contacts between the 4 domains (V $\alpha$ -V $\beta$ , V $\alpha$ -C $\alpha$ , V $\beta$ -C $\beta$ , and C $\alpha$ -C $\beta$ ) differ. Hence, the most stable binding mode between any two domains in isolation may be incompatible when they are embedded within the TCR $\alpha\beta$  heterodimer. Interfacial mismatch is exacerbated when TCR $\alpha\beta$  binds pMHC, which adds two more interfaces, namely V $\alpha$ -pMHC and V $\beta$ -pMHC. Without an adequate load, the mismatched interfaces lead to conformational motion of the individual domains, destabilizing the complex and shortening the bond lifetime. When a 10- to 20-pN load is applied, however, a slight deformation of the complex occurs, resulting in a better fit and stabilization of the interfaces (Fig. 4D). In this mechanism, the dominance of the contacts with the MHC molecule rather than with the peptide per se is required since the MHC must grab

and pull V $\alpha$  and V $\beta$  to suppress the motion. Instead, the peptide organizes the surrounding contacts, screening for the correct fit rather than bearing the load, akin to the teeth of a key that slot into a lock, while the key's stem bears the load when turning the key.

Allostery can naturally be incorporated into the proposed catch bond mechanism since changes in any of the 4 domains impact the interfacial dynamics. In particular, the C $\beta$  FG-loop that is present in jawed vertebrates (*gnathostomata*) and elongated in mammals (14), strongly influences stability of the TCR $\alpha\beta$ -pMHC complex. Our simulation showed that V $\beta$ -C $\beta$  form more extensive interdomain contacts compared to those of V $\alpha$ -C $\alpha$  where the C $\beta$  FG-loop controls the orientation of V $\beta$  relative to C $\beta$ , in addition to providing structural support for V $\alpha$  in binding to pMHC. In an FG-loop deletion mutant, the orientation and conformational motion of the V-module changes, destabilizing the interface with pMHC when load is applied (Fig. 4C). The proposed catch bond mechanism is also compatible with the 9 to 15-nm conformational transition observed experimentally. In simulations where the

C-module was removed (31), the interface between the V-module and pMHC became more stable than even the high-load case (Fig. 4E) due to absence of the C-module interfacial mismatch, allowing a better fit with pMHC. A partial unfolding of the C-module may occur in the extended state, keeping the V-module engaged with pMHC as the transition occurs. More studies are needed to characterize the structural origin of the conformational transition in TCR $\alpha\beta$ , information that in turn could lead to optimal TCR design for immunotherapy.

We recently analyzed load-dependence of another set of TCR $\alpha\beta$ -pMHC systems, involving the adult T cell leukemia A6 TCR and agonist and nonstimulatory peptides in complex with HLA-A\*0201 that were studied by X-ray crystallography in the past (51). Consistent with our previous MD study, the interface was stabilized upon application of physiological-level loads. In contrast, the presence of antagonist peptides led to destabilization of the complex with load, indicative of a slip bond behavior (53). These results suggest that the catch bond mechanism based on domain motion and interfacial mismatch is general, predicated on the basic organization of domain interfaces. We posit that the interaction with pMHC by preTCRs expressed on DN thymocytes and manifesting ligand-dependent catch bond formation speaks to the fundamental  $\alpha\beta$  thymic selection process. During TCR repertoire development, preTCRs may be screened not only for sequence-dependent interaction with self-pMHC, but also for proper mechanical matching.

### Impact of Force on TCR vs. BCR and CAR-T Systems

Structural analyses by cryo-electron microscopy of  $\alpha\beta$ TCRs (54–56) provide considerable insight into the features that imbue the receptor with its anisotropic (directed) mechanosensing involving the amalgam of CD3 subunits and force transduction architecture (SI Appendix, Text S3 and Fig. S2A). NMR data support that a dynamic TM segment conformational switch of the TCR $\alpha$  subunit impacts  $\alpha\beta$ TCR mechanotransduction as well as dissociation of the CD3 subunits

from TCR $\alpha\beta$  (25). Rapid dissociation of CD3 $\zeta\zeta$  is noteworthy, given its prominent role in CAR-T systems (SI Appendix, Fig. S3).

B cell receptor (BCR) structures have also been characterized, revealing a TM immunoglobulin molecule noncovalently associated with CD3-like Ig $\alpha/\beta$  heterodimeric signaling molecules (57–59) (SI Appendix, Text S4 and Fig. S2B). BCRs likewise detect force, utilizing cellular energy to discriminate ligand affinity (60), but without catch bond formation. Separation of ligand binding and signaling functions into distinct subunits and physical dissociation of those components from one another are common to both membrane-bound systems (SI Appendix, Texts S3 and S4).

Biophysical measurements of CAR-T cells show markedly different properties than  $\alpha\beta$  T cells interacting with the same pMHC ligands (SI Appendix, Text S5). As CAR-T cells and diabodies lack physiological TCR mechanotransduction features, the sensitivity of such systems is unsurprisingly less than that of digital  $\alpha\beta$ TCR mechanosensors (61). While CARs are strategically facile, they lack participation of the C $\beta$  loading pathway and the TCR $\alpha$  TM switch. They are also grossly unmatched to the typical lifetime and force ranges found in native TCR-pMHC interactions. Thus, there are opportunities for new CAR-T strategies given the potential for 1) coupling more directly to the same load pathway utilized in  $\alpha\beta$  T cells in fostering conformational transition, 2) matching more appropriately the force window for native T cell activation such that membrane, cytoskeletal machinery, and motors can participate optimally and 3) better mimicking the lifetime profile found in native T cells. Consistent with this notion, a recent study showed that HLA-independent T cell receptors (HITs), chimeric designs utilizing V $_H$ -V $_L$  module replacement of the V $\alpha$ -V $\beta$  module of the  $\alpha\beta$ TCR, can target tumors with low antigen density (SI Appendix, Fig. S1C) (62). Similar to the V $\gamma\delta$ -C $\alpha\beta$  chimera, HITs may possess a catch bond, and with the same C $\alpha\beta$ -module and CD3 signaling subunits as the  $\alpha\beta$ TCR complex, that promote conformational transitions and digital sensitivity to the low-density antigen. Further single-molecule (SM) and simulation studies will help to understand the mechanism of HITs.

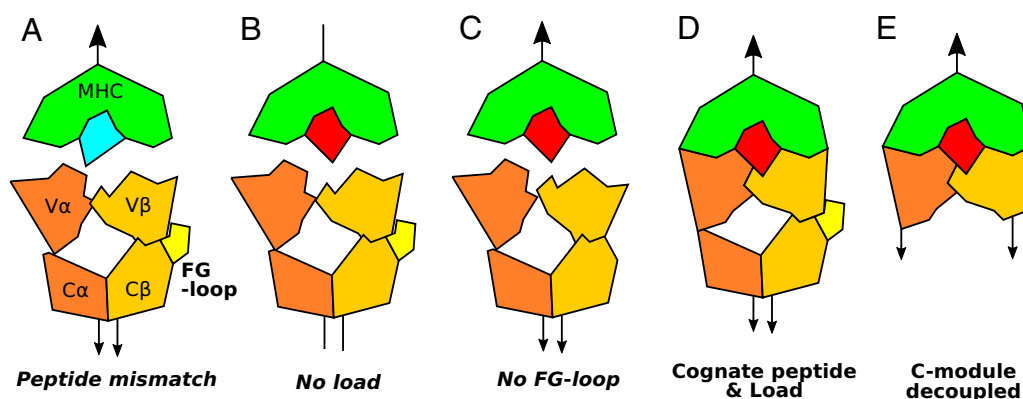


**Fig. 4.** Interdomain motions define an atomistic basis of  $\alpha\beta$ TCR-pMHC catch bond formation. (A) Nonmatching peptide, (B) absence of adequate load, or (C) deletion of the C $\beta$  FG-loop leads to mismatch between subdomains and allow domain motion, which lead to destabilization of the  $\alpha\beta$ TCR-pMHC interface. (D) When the complex with a cognate peptide is under 10- to 20-pN load, fit between domains is achieved, stabilizing the bond. (E) Decoupling between the V- and C-modules, as would occur in the extended state of the complex, eliminates the requirement to satisfy the V-C interface, which enhances the fit between the V-module and pMHC. In this illustration, interfacial matches are shown as geometric fit. In reality, it can be more subtle, such as matches in motional behavior. By incorporating “mechanical match,” the peptide discrimination can be enhanced far beyond chemical and conformational matches in equilibrium. See refs. 31 and 53 for MD simulations upon which the model is based.

## Implications of $\alpha\beta$ TCR Mechanobiology as Related to Tumor Antigen Targeting

Principles of mechanobiology suggest how to optimize T cell monitoring and craft effective immunotherapies. Force omission in in vitro immunological studies obscures  $\alpha\beta$  T cell recognition of sparse pMHC ligands including neoantigens or certain viral antigens. For effective immuno-oncology approaches, a match must exist between a CTL  $\alpha\beta$ TCR acuity, i.e., its ability to recognize a threshold number of pMHC complexes incorporating a neoantigen on a target cell, and the number of copies arrayed on that tumor. Pertinently, certain CTLs manifest digital performance whereas other CTLs need dozens or even hundreds of pMHC copies. If there is such a quantitative mismatch, then no killing of tumor will occur in vivo even if “specific” killing of peptide pulsed APCs in vitro is detected. Emphatically, the array on the actual tumor cell is relevant, not a surrogate APC that has been pulsed with micromolar concentrations of peptides yielding thousands of copies of a particular pMHC complex. A variety of evolving methods (microfluidics, smart particles, and optical tweezers) (10, 42, 43, 63–65) exert force on  $\alpha\beta$ TCR-pMHC bonds to foster in vitro TCR performance studies that can gauge acuity. For experimentalists, the challenge is to determine which parameters of  $\alpha\beta$ TCR mechanotransduction correlate best with TCR activation responses (Fig. 5).

T cells and their purified receptor-pMHC proteins can be probed using biophysical tools at the SM and SM single-cell (SMSC) levels. Optical trapping facilitates an interaction and provides measurements (detailed in Fig. 5) that directly reveal the strength and properties of the TCR $\alpha\beta$ -pMHC bond. At the SM level, a good TCR $\alpha\beta$ -pMHC pair readily forms interactions and “holds” for a few seconds under load. Bond lifetime distributions typically exhibits a catch bond type profile (rather than irrelevant slip bond) peaking at  $\sim 15$  pN, a force where one likely observes a conformational change. Good pairs show a clear conformational transition, and many will reversibly hop when held at the right force window. Parameters include lifetime, transition distance, critical force for hopping, and hopping frequency. While purified components provide the highest resolution measurements, similar studies can be performed directly on the surface of a coverslip-bound T cell, eliminating the need for protein expression and purification (SMSC in Fig. 5). Here pMHC is tethered to a bead through a DNA rope and brought in the vicinity of the cell by manipulating the optical trap or cell position. Repeat measurements reveal catch bond curves and even visible transitions. Although the data are “noisier” due to cell motions along the load pathway, one can readily score the ease of forming and maintaining interactions (and frequently identify conformational change) across a panel of cells. Perhaps the best test of cell’s quality against a particular peptide is an assay where one actually mimics activation by proxy through presentation of a bead (and associated force) to determine what physical and chemical thresholds are required for activation [SCAR (Single-cell activation requirement) in Fig. 5]. The measurement not only involves mechanical manipulation of the trap but also a simultaneous fluorescence measurement to track calcium flux

changes, a marker for early T cell activation. Parameters include chemical threshold for activation, force threshold for activation, calcium flux magnitude and rate, activation probability, and frequency of forming bead-cell adhesion. High-quality T cell-pMHC pairs can be triggered with as few as 2 molecules at the bead-cell interface. As only a few “bits” of information are processed by the cell, we refer to this as a digital activation. Digital T cells readily bind beads and show a steady and sustained rise in calcium in response to bead presentation.

Defining biomarkers that correlate with the above biophysical parameters of digital performance is a key next step. These signature molecules may include a set of differentially expressed activation molecules measurable using antibodies in conjunction with flow cytometry. Those molecules will likely be brought to light by in vivo single-cell RNAseq gene expression data derived from digital vs. analogue CD8 CTL performers directed at the same pMHC. How those biosignatures relate to IS formation and IS topology along with microtubule-organizing center polarization will also be interesting to discern. Readily measurable markers will circumvent the limited access of immunooncologists currently to detailed mechanobiological measurements.

The crucial task of neoantigen identification has been approached in several ways as identified in *SI Appendix, Text S6*. The recently developed attomole ( $10^{-18}$ ) Poisson detection liquid chromatography-data independent acquisition mass spectrometry (LC-DIAMS) method is an important step forward (66–68). It captures the entire immune peptidome in a single run from small numbers of tumor cells ( $10^6$ ) retrieved by clinical fine needle biopsy. This method uses a Poisson metric to detect a reference fragmentation pattern embedded in a background of ion fragments and mitigates false negative or false-positive detection (67). It meets the challenge of the complexity, limited sample, and spectral crowding of molecular ions and suits a focus on detecting very low abundance peptides from a very large number of candidate peptides that could mark the cell as infected or transformed. The advance changes the MS calculus, permitting neoantigen search at any point following data collection using existing MS instrumentation in a facile manner to detect both sparse and luminous targets. Both truncal mutations associated with all tumor cells of an individual as well as nontruncal clonal variants are detectable via LC-DIAMS from analysis of individual biopsy sites at one point in time or over the clinical course of a cancer. For CTL-based vaccines to prevent infectious diseases, there is opportunity to target viral, parasitic, or other infectious antigens that appear early in the infectious process after the pathogen’s entry into a host cell (69).

## Clinical Benefit Resulting from TCR Mechanobiology and Its Modulation

The matching of TCR mechanosensory performance with distinct neoantigen displays is likely to create a new dawn of immuno-oncology for personalized immunotherapies including targeting of certain high value truncal neoantigens such as TP53 shared by multiple patients (9). With respect to TAA, although these are not tumor-specific peptides given their expression on normal fetal or adult cell types, the array



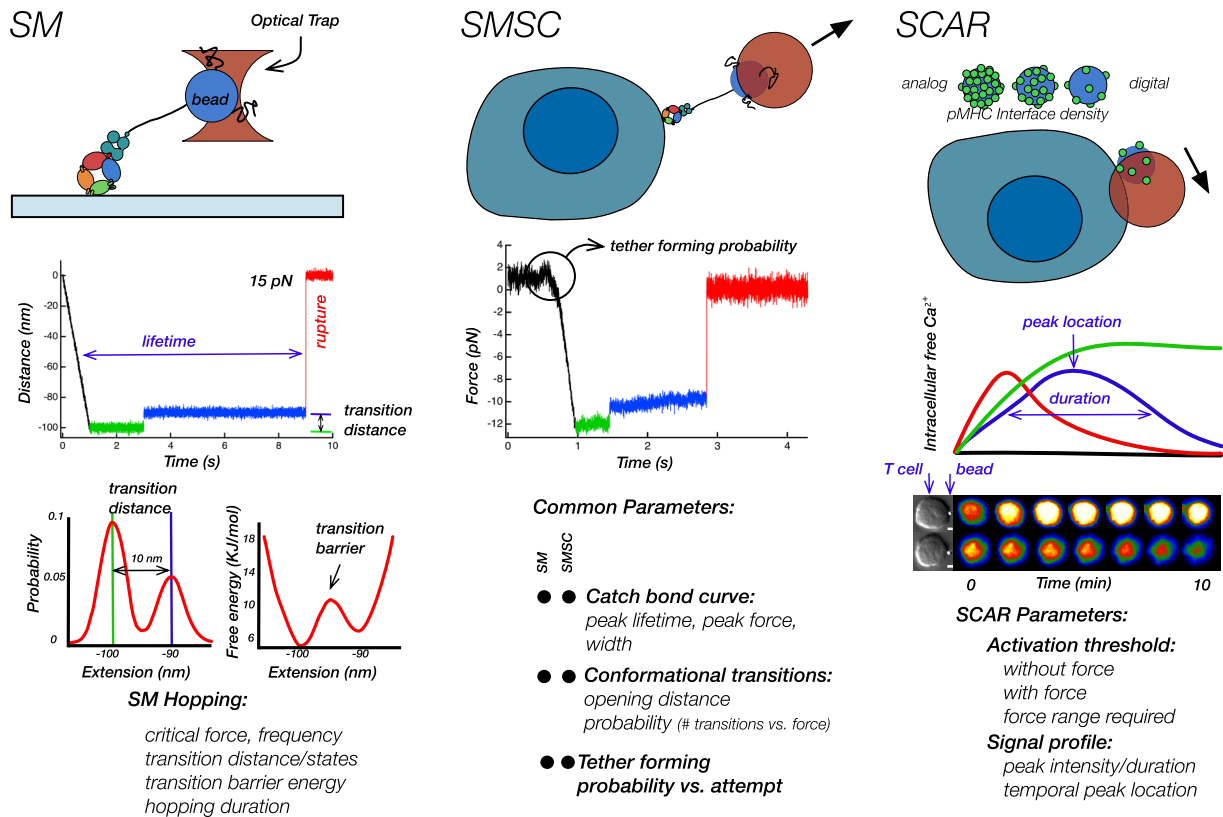


**Fig. 5.** Single-molecule biophysical parameters defining  $\alpha\beta$ TCR-pMHC recognition. (Left column) Single-molecule (SM) measurements probe purified TCR $\alpha\beta$ -pMHC interactions by loading the bond through an optically trapped bead with 0.1-pN force and nm-level spatial resolution. Multiple traces scoring bond lifetimes vs. force populate catch bond curves (example in Fig. 2B) yielding lifetime and force as well as shifts in catch bond profile width. At the critical force, reversible transitions can be tracked to obtain hopping frequency (Fig. 2D), hopping distance, and transition barrier energetics. (Middle) Single-molecule single-cell (SMSC) measurements by tethering pMHC molecules to a bead and presenting the bead to a surface-bound T cell. When the tethered bead is pulled away, it produces a transient that can score the bond lifetime for a given force (catch bond curves), transition magnitudes, and opening probabilities for a given force window. (Right) Single-cell activation requirement (SCAR) measurements by trapping a pMHC-coated bead and facilitating interfacial contact with a T cell containing a fluorescence-based reporter of calcium concentration. Beads of varying pMHC densities ranging from analog to digital are presented to determine the interfacial copy number required for activation with and without force. At limiting pMHC, force is required for activation (digital). In this case the optical trap is not only used to facilitate bead connection with the cell, but force on the bead pulls on the pMHC-TCR bond mimicking a shear load between the T Cell and APC across such a bond through their respective actomyosin machineries. Such force is expected to lead to a conformational change in the TCR including reversible transitioning, which agitates the membrane sequestered ITAM domains releasing them and leading to changes in phosphorylation. Intracellular calcium flux transients show a range of profiles from nonactivating (black) to activating (blue and red) and sustained (green) (11). A 10-min time course showing activating (Top) and nonactivating (Bottom) cells are shown. Differential interference contrast images are shown on the left with a 1- $\mu$ m bead and scale bar. For simplicity, the SMSC model lacks CD3 components of the cell surface  $\alpha\beta$ TCR complex while the SCAR model omits TCRs altogether.

of certain TAA across tissues and cell types can be very limited in distribution while highly overexpressed on tumors. This differential expression profile creates a therapeutic opportunity. The anaplastic lymphoma kinase (ALK) is an example where TAA epitope-specific T cells can be engendered against ALK without central tolerance (70). The potential to convert physically defined but immunologically weak TAA into strongly immunogenic TAA has been documented through clever structural analyses offering additional future therapeutic vaccination opportunities (71).

Some investigators have begun to exploit mechanobiology to identify TCRs with enhanced TCR-pMHC catch bonds through site-directed mutagenesis of the specific TCR-ligand interaction surface (28). This approach seeks to avoid cross-reactivity against off-target antigens as previously resulted in fatal organ immunopathology and occurred through engineering of TCRs for antibody-like high-affinity TAA recognition in the absence of force. It is presently unclear whether enhanced catch bond formation alone shall be broadly successful in avoiding such a danger. Many additional TCR

biophysical parameters exist (Figs. 2 and 5), requiring exploration to identify the best surrogates of TCR performance and specificity. Without a nuanced appreciation of mechanobiology, serious errors may follow. Recent usage of an TCR $\beta$  CAR-T with an unpaired  $V\alpha$  touted as an efficient way to achieve TAA targeting would result in significant peptide cross-reactivities akin to a preTCR as evidenced by activation without peptide addition (72).

As a more global approach to discern CTL performance predicated on TCR mechanobiology, repertoires of T cells recognizing a single ligand (viral- or tumor-related) should yield important information. The sequence relatedness of highly functional T cells, associations with immune protection, inflammatory pathologies, damaging cross-reactivities with other self-derived epitopes in tissues, and propensities to progress to exhaustion, can all be explored. Not all T cells bearing different TCR clonotypes respond in the same manner against a virally infected or transformed cell. Within such a single pMHC-specific repertoire, the determination of TCR sequence distance, differential MD simulation behavior,

structural features, biological performance in vivo as well as in vitro, and transcriptomes in response to pMHC ligand shall inform us about the hallmarks of optimal performance to guide adoptive  $\alpha$ T cell therapy. In turn, investigators can vet epitopes for incorporation into cancer vaccines to induce T cells arraying optimal cognate recognition receptors.

**Data, Materials, and Software Availability.** All study data are included in the article and/or *SI Appendix*.

**ACKNOWLEDGMENTS.** We gratefully acknowledge members of the Reinherz, Hwang, and Lang Labs for helpful comments and feedback on the manuscript and Kemin Tan for assistance with graphics. This work is supported by NIH P01 Grant AI143565 and NIH R01 grant AI136301 to E.L.R., W.H., and M.J.L.

1. P. Sharma *et al.*, The next decade of immune checkpoint therapy. *Cancer Discov.* **11**, 838–857 (2021).
2. M. Yarchoan, A. Hopkins, E. M. Jaffee, Tumor mutational burden and response rate to PD-1 inhibition. *N. Engl. J. Med.* **377**, 2500–2501 (2017).
3. N. R. Mahadevan *et al.*, Intrinsic immunogenicity of small cell lung carcinoma revealed by its cellular plasticity. *Cancer Discov.* **11**, 1952–1969 (2021).
4. S. K. Kim, S. W. Cho, The evasion mechanisms of cancer immunity and drug intervention in the tumor microenvironment. *Front. Pharmacol.* **13**, 868695 (2022).
5. S. Kitajima *et al.*, MPS1 inhibition primes immunogenicity of KRAS-LKB1 mutant lung cancer. *Cancer Cell* **40**, 1128–1144.e8 (2022).
6. S. Qin *et al.*, Novel immune checkpoint targets: Moving beyond PD-1 and CTLA-4. *Mol. Cancer* **18**, 155 (2019).
7. I. Chmielewska, K. Stencel, E. Kalinka, R. Ramlau, P. Krawczyk, Neoadjuvant and adjuvant immunotherapy in non-small cell lung cancer-clinical trials experience. *Cancers (Basel)* **13**, 5048 (2021).
8. R. M. Young, N. W. Engel, U. Uslu, N. Wellhausen, C. H. June, Next-generation CAR T-cell therapies. *Cancer Discov.* **12**, 1625–1633 (2022).
9. E. H. Hsue *et al.*, Targeting a neoantigen derived from a common TP53 mutation. *Science* **371**, eabc8697 (2021).
10. Y. Feng *et al.*, Mechanosensing drives acuity of alphabeta T-cell recognition. *Proc. Natl. Acad. Sci. U.S.A.* **114**, E8204–E8213 (2017).
11. Y. Feng, E. L. Reinherz, M. J. Lang, alphabeta T cell receptor mechanosensing forces out serial engagement. *Trends Immunol.* **39**, 596–609 (2018).
12. R. J. Mallis *et al.*, Molecular design of the gammadelta T cell receptor ectodomain encodes biologically fit ligand recognition in the absence of mechanosensing. *Proc. Natl. Acad. Sci. U.S.A.* **118**, e2023050118 (2021).
13. M. J. Walsh, M. Dougan, Checkpoint blockade toxicities: Insights into autoimmunity and treatment. *Semin. Immunol.* **52**, 101473 (2021).
14. J. H. Wang, E. L. Reinherz, The structural basis of alphabeta T-lineage immune recognition: TCR docking topologies, mechanotransduction, and co-receptor function. *Immunol. Rev.* **250**, 102–119 (2012).
15. R. Andargachew, R. J. Martinez, E. M. Kolawole, B. D. Evavold, CD4 T cell affinity diversity is equally maintained during acute and chronic infection. *J. Immunol.* **201**, 19–30 (2018).
16. D. B. Keskin *et al.*, Direct identification of an HPV-16 tumor antigen from cervical cancer biopsy specimens. *Front. Immunol.* **2**, 75 (2011).
17. T. Sasada, Y. Ghendler, J. H. Wang, E. L. Reinherz, Thymic selection is influenced by subtle structural variation involving the p4 residue of an MHC class I-bound peptide. *Eur. J. Immunol.* **30**, 1281–1289 (2000).
18. D. Nemazee, Mechanisms of central tolerance for B cells. *Nat. Rev. Immunol.* **17**, 281–294 (2017).
19. T. K. Starr, S. C. Jameson, K. A. Hogquist, Positive and negative selection of T cells. *Annu. Rev. Immunol.* **21**, 139–176 (2003).
20. U. Storb *et al.*, Molecular aspects of somatic hypermutation of immunoglobulin genes. *Cold Spring Harb. Symp. Quant. Biol.* **64**, 227–234 (1999).
21. Y. Sykulev, M. Joo, I. Vturina, T. J. Tsomides, H. N. Eisen, Evidence that a single peptide-MHC complex on a target cell can elicit a cytolytic T cell response. *Immunity* **4**, 565–571 (1996).
22. D. K. Das *et al.*, Force-dependent transition in the T-cell receptor beta-subunit allosterically regulates peptide discrimination and pMHC bond lifetime. *Proc. Natl. Acad. Sci. U.S.A.* **112**, 1517–1522 (2015).
23. S. T. Kim *et al.*, The alphabeta T cell receptor is an anisotropic mechanosensor. *J. Biol. Chem.* **284**, 31028–31037 (2009).
24. D. K. Das *et al.*, Pre-T cell receptors (Pre-TCRs) leverage Vbeta complementarity determining regions (CDRs) and hydrophobic patch in mechanosensing thymic self-ligands. *J. Biol. Chem.* **291**, 25292–25305 (2016).
25. K. N. Brazin *et al.*, The T cell antigen receptor alpha transmembrane domain coordinates triggering through regulation of bilayer immersion and CD3 subunit associations. *Immunity* **49**, 829–841.e6 (2018).
26. D. Banik *et al.*, Single molecule force spectroscopy reveals distinctions in key biophysical parameters of alphabeta T-cell receptors compared with chimeric antigen receptors directed at the same ligand. *J. Phys. Chem. Lett.* **12**, 7566–7573 (2021).
27. B. Liu, W. Chen, B. D. Evavold, C. Zhu, Accumulation of dynamic catch bonds between TCR and agonist peptide-MHC triggers T cell signaling. *Cell* **157**, 357–368 (2014).
28. X. Zhao *et al.*, Tuning T cell receptor sensitivity through catch bond engineering. *Science* **376**, eabl5282 (2022).
29. P. Wu *et al.*, Mechano-regulation of peptide-MHC class I conformations determines TCR antigen recognition. *Mol. Cell* **73**, 1015–1027.e7 (2019).
30. A. K. Chakraborty, A. Weiss, Insights into the initiation of TCR signaling. *Nat. Immunol.* **15**, 798–807 (2014).
31. W. Hwang, R. J. Mallis, M. J. Lang, E. L. Reinherz, The alphabetaTCR mechanosensor exploits dynamic ectodomain allostery to optimize its ligand recognition site. *Proc. Natl. Acad. Sci. U.S.A.* **117**, 21336–21345 (2020).
32. J. J. Hopfield, Kinetic proofreading: A new mechanism for reducing errors in biosynthetic processes requiring high specificity. *Proc. Natl. Acad. Sci. U.S.A.* **71**, 4135–4139 (1974).
33. M. J. Shannon, G. Burn, A. Cope, G. Cornish, D. M. Owen, Protein clustering and spatial organization in T-cells. *Biochem. Soc. Trans.* **43**, 315–321 (2015).
34. T. Kreslavsky *et al.*, beta-Selection-induced proliferation is required for alphabeta T cell differentiation. *Immunity* **37**, 840–853 (2012).
35. X. Li *et al.*, Pre-T cell receptors topologically sample self-ligands during thymocyte beta-selection. *Science* **371**, 181–185 (2021).
36. R. J. Mallis, H. Arthanari, M. J. Lang, E. L. Reinherz, G. Wagner, NMR-directed design of pre-TCRbeta and pMHC molecules implies a distinct geometry for pre-TCR relative to alphabetaTCR recognition of pMHC. *J. Biol. Chem.* **293**, 754–766 (2018).
37. R. J. Mallis *et al.*, Pre-TCR ligand binding impacts thymocyte development before alphabetaTCR expression. *Proc. Natl. Acad. Sci. U.S.A.* **112**, 8373–8378 (2015).
38. J. S. Duke-Cohan *et al.*, Pre-T cell receptor self-MHC sampling restricts thymocyte differentiation. *Nature* **613**, 565–574 (2022), 10.1038/s41586-022-05555-7.
39. C. D. Castro, C. T. Boughter, A. E. Broughton, A. Ramesh, E. J. Adams, Diversity in recognition and function of human gammadelta T cells. *Immunol. Rev.* **298**, 134–152 (2020).
40. T. Wu *et al.*, Quantification of epitope abundance reveals the effect of direct and cross-presentation on influenza CTL responses. *Nat. Commun.* **10**, 2846 (2019).
41. J. Husson, K. Chemin, A. Bohineust, C. HIVroz, N. Henry, Force generation upon T cell receptor engagement. *PLoS One* **6**, e19680 (2011).
42. K. H. Hu, M. J. Butte, T cell activation requires force generation. *J. Cell Biol.* **213**, 535–542 (2016).
43. Y. Liu *et al.*, DNA-based nanoparticle tension sensors reveal that T-cell receptors transmit defined pN forces to their antigens for enhanced fidelity. *Proc. Natl. Acad. Sci. U.S.A.* **113**, 5610–5615 (2016).
44. H. Colin-York *et al.*, Cytoskeletal control of antigen-dependent T cell activation. *Cell Rep.* **26**, 3369–3379.e5 (2019).
45. K. T. Bashour *et al.*, CD28 and CD3 have complementary roles in T-cell traction forces. *Proc. Natl. Acad. Sci. U.S.A.* **111**, 2241–2246 (2014).
46. R. Basu *et al.*, Cytotoxic T cells use mechanical force to potentiate target cell killing. *Cell* **165**, 100–110 (2016).
47. K. L. Hui, L. Balagopalan, L. E. Samelson, A. Upadhyaya, Cytoskeletal forces during signaling activation in Jurkat T-cells. *Mol. Biol. Cell* **26**, 685–695 (2015).
48. J. Huang *et al.*, Extracellular matrix and its therapeutic potential for cancer treatment. *Signal Transduct. Target Ther.* **6**, 153 (2021).
49. H. Du *et al.*, Tuning immunity through tissue mechanotransduction. *Nat. Rev. Immunol.* **23**, 174–188 (2022), 10.1038/s41577-022-00761-w.
50. T. R. Cox, J. T. Ertler, Remodeling and homeostasis of the extracellular matrix: Implications for fibrotic diseases and cancer. *Dis. Model Mech.* **4**, 165–178 (2011).
51. Y. H. Ding, B. M. Baker, D. N. Garboczi, W. E. Biddison, D. C. Wiley, Four A6-TCR/peptide/HLA-A2 structures that generate very different T cell signals are nearly identical. *Immunity* **11**, 45–56 (1999).
52. B. Liu, E. M. Kolawole, B. D. Evavold, Mechanobiology of T cell activation: To catch a bond. *Annu. Rev. Cell Dev. Biol.* **37**, 65–87 (2021).
53. A. C. Chang-Gonzalez, R. J. Mallis, M. J. Lang, E. L. Reinherz, W. Hwang, Load-dependent conformational behavior of the A6 TCR HLA-A2/Tax pMHC complex. *Biophys. J.* **121**, 145A (2022), 10.1016/j.bpj.2021.11.1999.
54. Dong *et al.*, Structural basis of assembly of the human T cell receptor-CD3 complex. *Nature* **573**, 546–552 (2019).
55. Y. Chen *et al.*, Cholesterol inhibits TCR signaling by directly restricting TCR-CD3 core tunnel motility. *Mol. Cell* **82**, 1278–1287.e5 (2022).
56. L. Susac *et al.*, Structure of a fully assembled tumor-specific T cell receptor ligated by pMHC. *Cell* **185**, 3201–3213.e19 (2022).
57. Q. Su *et al.*, Cryo-EM structure of the human IgM B cell receptor. *Science* **377**, 875–880 (2022).
58. X. Ma *et al.*, Cryo-EM structures of two human B cell receptor isotypes. *Science* **377**, 880–885 (2022).
59. Y. Dong *et al.*, Structural principles of B cell antigen receptor assembly. *Nature* **612**, 156–161 (2022), 10.1038/s41586-022-05412-7.
60. E. Natkanski *et al.*, B cells use mechanical energy to discriminate antigen affinities. *Science* **340**, 1587–1590 (2013).
61. A. I. Salter *et al.*, Comparative analysis of TCR and CAR signaling informs CAR designs with superior antigen sensitivity and in vivo function. *Sci. Signal* **14**, eabe2606 (2021).
62. J. Mansilla-Soto *et al.*, HLA-independent T cell receptors for targeting tumors with low antigen density. *Nat. Med.* **28**, 345–352 (2022).
63. Y. C. Li *et al.*, Cutting Edge: Mechanical forces acting on T cells immobilized via the TCR complex can trigger TCR signaling. *J. Immunol.* **184**, 5959–5963 (2010).
64. P. Robert *et al.*, Kinetics and mechanics of two-dimensional interactions between T cell receptors and different activating ligands. *Biophys. J.* **102**, 248–257 (2012).
65. Y. Feng, X. Zhao, A. K. White, K. C. Garcia, P. M. Fordyce, A bead-based method for high-throughput mapping of the sequence- and force-dependence of T cell activation. *Nat. Methods* **19**, 1295–1305 (2022).
66. S. L. Wickstrom *et al.*, Cancer neopeptides for immunotherapy: Discordance between tumor-infiltrating T cell reactivity and tumor mhc peptidome display. *Front. Immunol.* **10**, 2766 (2019).
67. B. Reinhold, D. B. Keskin, E. L. Reinherz, Molecular detection of targeted major histocompatibility complex I-bound peptides using a probabilistic measure and nanospray MS3 on a hybrid quadrupole-linear ion trap. *Anal. Chem.* **82**, 9090–9099 (2010).
68. D. B. Keskin *et al.*, Physical detection of influenza A epitopes identifies a stealth subset on human lung epithelium evading natural CD8 immunity. *Proc. Natl. Acad. Sci. U.S.A.* **112**, 2151–2156 (2015).
69. S. Sengupta *et al.*, TCR-mimic bispecific antibodies to target the HIV-1 reservoir. *Proc. Natl. Acad. Sci. U.S.A.* **119**, e2123406119 (2022).
70. C. Voena *et al.*, Efficacy of a cancer vaccine against ALK-rearranged lung tumors. *Cancer Immunol. Res.* **3**, 1333–1343 (2015).
71. P. Wei *et al.*, Structures suggest an approach for converting weak self-peptide tumor antigens into superagonists for CD8 T cells in cancer. *Proc. Natl. Acad. Sci. U.S.A.* **118**, e2100588118 (2021).
72. J. Oh *et al.*, Single variable domains from the T cell receptor beta chain function as mono- and bifunctional CARs and TCRs. *Sci. Rep.* **9**, 17291 (2019).